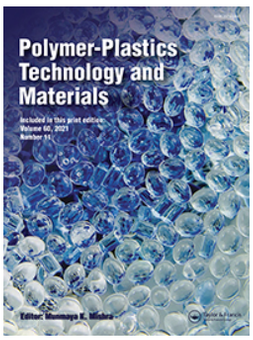

Polymer-Plastics Technology and Materials

ISSN: (Print) (Online) Journal homepage: https://www.tandfonline.com/loi/lpte21

# The Comprehensive study of Titanium oxide doped Conducting polymers nanocomposites for Photovoltaic applications

Bhagyashri U. Tale, K. R. Nemade & P. V. Tekade

**To cite this article:** Bhagyashri U. Tale, K. R. Nemade & P. V. Tekade (2021): The Comprehensive study of Titanium oxide doped Conducting polymers nanocomposites for Photovoltaic applications, Polymer-Plastics Technology and Materials, DOI: 10.1080/25740881.2021.1930047

**To link to this article:** https://doi.org/10.1080/25740881.2021.1930047

Published online: 31 May 2021.

POLYMER-PLASTICS TECHNOLOGY AND MATERIALS
https://doi.org/10.1080/25740881.2021.1930047



# The Comprehensive study of Titanium oxide doped Conducting polymers nanocomposites for Photovoltaic applications

Bhagyashri U. Tale[a], K. R. Nemade[b], and P. V. Tekade[a]

[a]Department of Chemistry, Bajaj College of Science, Wardha, India; [b]Department of Physics, Indira Mahavidyalaya, Kalamb, India

**ABSTRACT**

To make the effective use of renewable energy, high performance, low-cost, and eco-friendly energy conversion devices are topic of intense research. Effect of addition of $TiO_2$ on photovoltaic performance of polymers was studied. The significant enhancement in % η was observed after addition of $TiO_2$ in Polyaniline. The Titanium dioxide ($TiO_2$) is n-type semiconductor with mechanical flexibility, and its conductivity can be modified by doping with PANi (*p*-type) to obtain high current by exciton separation at $TiO_2$/PANi interface. The value of % η (10.47%) for $TiO_2$-Polyaniline composite is found to be highest.

**ARTICLE HISTORY**
Received 14 April 2021
Revised 3 May 2021
Accepted 11 May 2021

**KEYWORDS**
Nano-composites; solar cells; supercapacitors

## 1. Introduction

The energy requirement of world is rising day by day and it is estimated that energy requirement will be double by 2050.[1] A photovoltaic or solar cell is used to convert the light energy into electrical energy. The electric power generation from renewable energy sources is the need of time. Among renewable energy resources used for generation of electricity, solar photovoltaic technology is rapidly growing.[2,3]

The interesting characteristics for the replacement of traditional energy sources by photovoltaic technology are

- Fossil fuels are limited and their cost is increasing day by day on the other hand solar energy is abundant & free.
- Fossil-fuels pollute the environment & solar PV's does not release pollutants.
- Fossil-fuels create global warming & solar PV's does not.
- As compared to other renewable energy sources, solar PV's provide the highest power density.
- Solar PV's has low operational costs & maintenance.
- There are more than 100 countries in the world where the work on solar PV technology is topic of intense research.[4–10]

### 1.1. Metal oxide/polymer composites

Polymer solar cells work in the following four stages for photocurrent generation:

(1) Excitons formation by absorption of light by the activated layer.

(2) Free charges formation by excitons at electron donor/acceptor interface.

(3) Transfer of the charged species in presence of electric field.

(4) Collection of charge by electrodes.[11]

One of the popular methods for charge separation in organic films is the addition of electron acceptors like $TiO_2$nanomaterial.[12,13]Polymer/inorganic composite is topic of interest in research due to the synergetic effects which lead to better electrical properties. The direct interfacial interaction of the polymers &inorganic component in composite improves electronic properties. In composite, the polymeric material acts as donors and inorganic component are acceptors.

In this study, Titanium dioxide ($TiO_2$) is n-type semiconductor with mechanical flexibility, and its conductivity can be modified by doping with PANi (*p*-type) to obtain high current by exciton separation at $TiO_2$ /PANiinterface.[14–17] Polyaniline is one of the most studied material because of its eco-friendliness, good electrical conductivity, low cost, rigidity, unique reversible protonic dupability etc. PANI is widely used in nanoelectronic devices.

The high efficiency of composites of PANi&$TiO_2$in photovoltaic devices can be explained on the basis of following:

1. The band-gap energies of PANI (2.8 eV) &$TiO_2$ (3.2 eV) are nearly same which facilitates the separation of charges and the transfer of electrons.

**CONTACT** Bhagyashri U. Tale bhagyashritale@gmail.com Department of Chemistry, Bajaj College of Science, Wardha, Maharashtra, India

2. The photo-generated electrons get excited by light which increases the conductivity as well as photoelectrochemical response.

Another reason for enhanced photosensitivity of PANI/$TiO_2$ film depends on energy level. When PANI/$TiO_2$film irradiates withlight, boththe$TiO_2$ and PANI shows absorption of photons & charge separation. As the conduction band of $TiO_2$ and the LUMO level of the PANI are nearer to each other, it facilitates the charge transfer.[18,19]

## 2. Experimental

In present work, Polyaniline (PANi) was prepared by Chemical oxidative method by Ammonium persulfate as oxidant. Both aniline and oxidant in stoichiometric ratio were dissolved in aqueous medium. The greenish black ppt was obtained and it was kept for 24 hours at room temperature to achieve complete polymerization. The product was washed with distilled water and then dried in an oven.[20] For preparation of Polypyrrole(PPy), $FeCl_3$ was used as oxidizing agent. The suspension was kept at room temperature for 24 hours to get complete polymerization. Finally, the black ppt. of polypyrrole was washed with Acetone and dried in an oven.[21]

Polyindole(PIn) was synthesized by Chemical oxidative method using $FeCl_3$ as an oxidizing agent and 0.1 M Hydrogen peroxide was added to enhance the rate of reaction. The reaction mixture was stirred for 12 hours at 30°C.[22] Polythiophene (PTh) was obtained by mixing thiophene with ferric chloride. Hydrogen peroxide was added to increase the rate of reaction. The complete polymerization was obtained by constant stirring for 24 hours at 30°C. Then, concentrated sodium hydroxide solution was added to get the product. The product was washed with distilled water and dried in oven.[23]

The Titanium dioxide ($TiO_2$) was obtained using 10% titanium chloride ($TiCl_3$), 15% HCl and ammonia solution in aqueous solution at alkaline pH. 3% $H_2O_2$was added to increase oxidation rate. The resulting solution was kept at room temperature for 24 hours and probe sonicated. The product was washed with distilled water and dried in oven.[24]The Polymer/Metal oxide composites were prepared by ex-situ approach. During preparation of composite, Polymer (1 g) and Metal oxide (0.1 g) were added to the organic media.

The X-ray diffraction (XRD) patterns of as prepared materials were recorded on Rigaku Miniflex-II X-Ray Diffractometer. The morphology of samples was investigated using scanning electron microscope (SEM) images obtained from JEOL JSM-7500 F. The ultraviolet–visible (UV–VIS) absorption spectra of composites were acquired using Agilent Cary 60 UV–VIS spectrophotometer. The Bruker RFS 27 Raman spectrometer was used for Raman analysis. Electrochemical study of prepared samples was carried out using three-electrode cell systems (CHI 660 D, CH Instruments). As-prepared materials were used as the working electrode, platinum wire as counter electrode and Ag/AgCl as the reference electrode. Photoluminescence (PL) spectra recorded using fluorescence spectroscopy (FL spectrophotometer model F-7000; Hitachi).

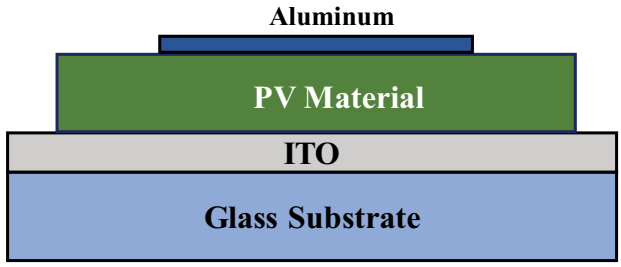


**Figure 1.** Side face of fabricated PV cell.

### 2.1. Fabrication of photovoltaic cell

The PV cells were prepared by doctor blade technique. The composite material was present as sandwich between ITO layer of plate and aluminum (Figure 1). The foil of aluminum acts as metallic electrode. The temporary binder was used to deposit the composite material on ITO coated plate and on that layer aluminum foil was kept. Then, it was dried at 40°C in order to remove the volatile organic components. The thickness of deposited layer was controlled by using transparency in doctor blade technique.

The current-voltage, that is, I–Vstudy of Photovoltaic cell was done by using an incandescent light bulb having power 0.2956 Watt/$m^2$. The parameters like short circuit current ($I_{SC}$), fill factor (FF), power conversion efficiency (η) & open-circuit voltage ($V_{OC}$) were measured using these conditions. The Fill Factor of Photovoltaic cell was measured using following equation,

$$FF = \frac{I_{MAX} \times V_{MAX}}{I_{SC} \times V_{OC}}$$

The power conversion efficiency, that is, %η of Photovoltaic cell was calculated by following relation,

$$\%\eta = \left(\frac{I_{SC} \times V_{OC} \times FF}{P_{in}}\right) \times 100$$

The FF and %η are the very important parameters for study of any PV cell. By using these parameters, it is possible to study any photovoltaic cell and its performance.

## 3. Result & discussion

### 3.1. XRD

Figure 2 indicates XRD pattern of (a) $TiO_2$, (b) Polyaniline (PANi), (c) Polythiophene (PTh), (d) Polypyrrole (PPy), (e) Polyindole (Pin), (f) $TiO_2$-Polyaniline composite (Ti-PANi), (g) $TiO_2$-Polythiophene composite (Ti-PTh), (h) $TiO_2$-Polypyrrole composite (Ti-PPy) and (i) $TiO_2$-Polyindole composite (Ti-Pin).

The experimental XRD pattern of $TiO_2$matches with the JCPDS card no. 21–1272 (anatase $TiO_2$). Strong diffraction peaks at 25°,38°, 48°, and 54° indicates $TiO_2$ in the anatase phase. The intensity of XRDpeaks indicates that the formed nanoparticles are crystalline.[25,26] X-ray diffraction of PANI shows peaks in the 2θ range 15° to 30°. The sharp and well-defined peaks indicate semi-crystalline nature of PANI. The crystalline nature of PANI is because of its nano fibrous nature and planarity of Benzenoid and Quinoid functional groups.[27]

XRD spectra of Polythiophene with only one broad peak centered at near 2θ value of 35°. This diffraction peak is due to π-π stacking structure in polythiophene chains. Thus, spectrum indicates the semi-crystalline nature of polythiophene.[28] The XRD pattern of Polyindole (PIn) shows a broad hump which indicates an amorphous structure which is the characteristic of Polyindole.[22] It is observed from the XRD of polypyrrole indicates its amorphous nature, as there is no sharp peak in the diffraction pattern. But a broad peak at about 24° of 2θ value is the characteristics peak of amorphous PPy polymer.[29]

Further the absence of broad diffraction peak of PANi at 2θ = 25° in the PANi/$TiO_2$ composite is due to the presence of PANi in the polymerization system which strongly affects the degree of crystallinity of $TiO_2$.[30] Similarly, crystalline behavior is found to be decrease with composite formation. Thus, the XRD pattern of $TiO_2$-Polyaniline composite (Ti-PANi), $TiO_2$-Polyindole composite(Ti-PIn), $TiO_2$-Polypyrrole

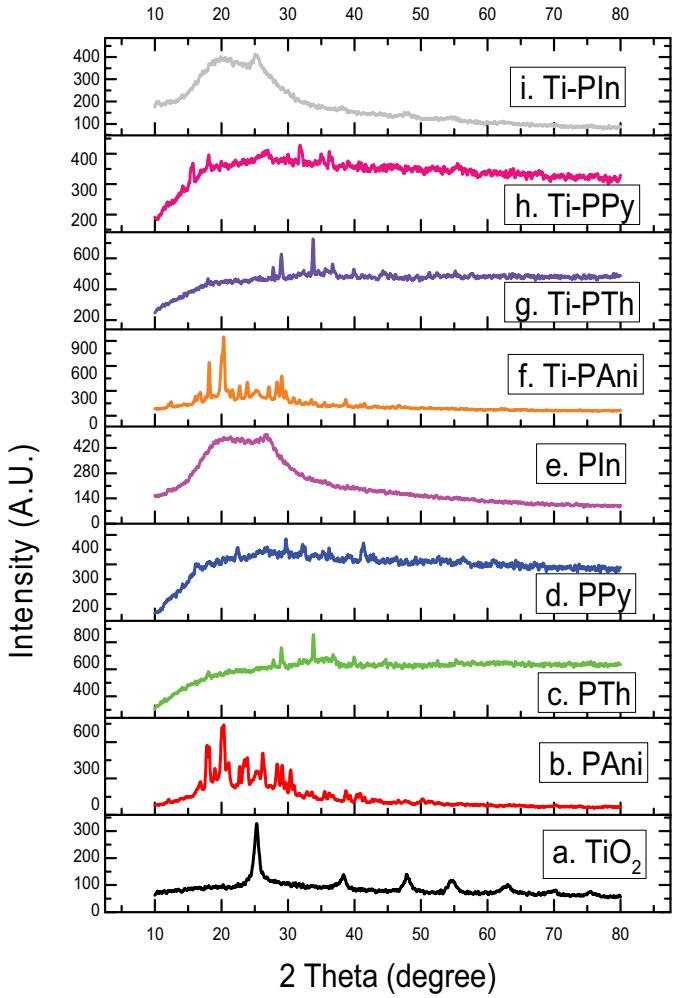


**Figure 2.** XRD pattern of (a) $TiO_2$, (b) Polyaniline (PANi), (c) Polythiophene (PTh), (d) Polypyrrole (PPy), (e) Polyindole (Pin), (f) $TiO_2$-Polyaniline composite (Ti-PANi), (g) $TiO_2$-Polythiophene composite (Ti-PTh), (h) $TiO_2$-Polypyrrole composite (Ti-PPy) and (i) $TiO_2$-Polyindole composite (Ti-Pin).

composite(Ti-PPy) and $TiO_2$-Polythiophene composite (Ti-PTh) indicates amorphous nature as there is no sharp peak.

Particle size of $TiO_2$, Polymers and their composites calculated by Scherrer equation are shown in Table 1.

**Table 1.** Particle size of $TiO_2$, polymers and their composites.

| Compound | Observed particle size calculated by Scherrer equation $D(nm) = K\lambda/\beta Cos\theta$[31] |
|---|---|
| 1. $TiO_2$, | 92.74 |
| 2. Polyaniline(PANi), | 84 |
| 3. Polythiophene(PTh), | 108.51 |
| 4. Polypyrrole (PPy), | 108.13 |
| 5. Polyindole(Pin), | 10.28 |
| 6. $TiO_2$-Polyaniline composite(Ti-PANi), | 165 |
| 7. $TiO_2$-Polythiophene composite(Ti-PTh), | 90.67 |
| 8. $TiO_2$-Polypyrrole composite(Ti-PPy) and | 50.67 |
| 9. $TiO_2$-Polyindole composite(Ti-Pin). | 8 |

### 3.2. SEM

SEM images of (a) $TiO_2$, (b) Polyaniline (PANi), (c) Polythiophene (PTh), (d) Polypyrrole (PPy), (e) Polyindole (Pin), (f) $TiO_2$-Polyaniline composite (Ti-PANi), (g) $TiO_2$-Polythiophene composite (Ti-PTh), (h) $TiO_2$-Polypyrrole composite (Ti-PPy) and (i) $TiO_2$-Polyindole composite (Ti-Pin) are shown in Figure 3.

### 3.3. Raman spectroscopy

Raman Spectra of(a) $TiO_2$, (b) Polyaniline (PANi), (c) Polythiophene (PTh), (d) Polypyrrole (PPy), (e) Polyindole (Pin), (f) $TiO_2$-Polyaniline composite (Ti-PANi), (g) $TiO_2$-Polythiophene composite (Ti-PTh), (h) $TiO_2$-Polypyrrole composite (Ti-PPy) and (i) $TiO_2$-Polyindole composite (Ti-PIn) are shown in Figure 4.

$TiO_2$ peak at 235 is due to rutile phase.[32,33] Raman spectra of Polyaniline indicates signal at 1140, 1230,1500 and 1582 $cm^{-1}$. 1100–1210 $cm^{-1}$ region is due to C–H bending vibrations of benzene or quinone type rings. 1210–1520 $cm^{-1}$ region indicates C-N stretching vibrations and 1520–1650 $cm^{-1}$ region denotes C–C stretching vibration of benzene and quinone type rings.[34]

Polythiophene shows sharp signal at 1209,1379 and 1651 $cm^{-1}$. Peak near 1600 $cm^{-1}$ indicates unquestionably frequency dispersion with increasing chain length. Signal

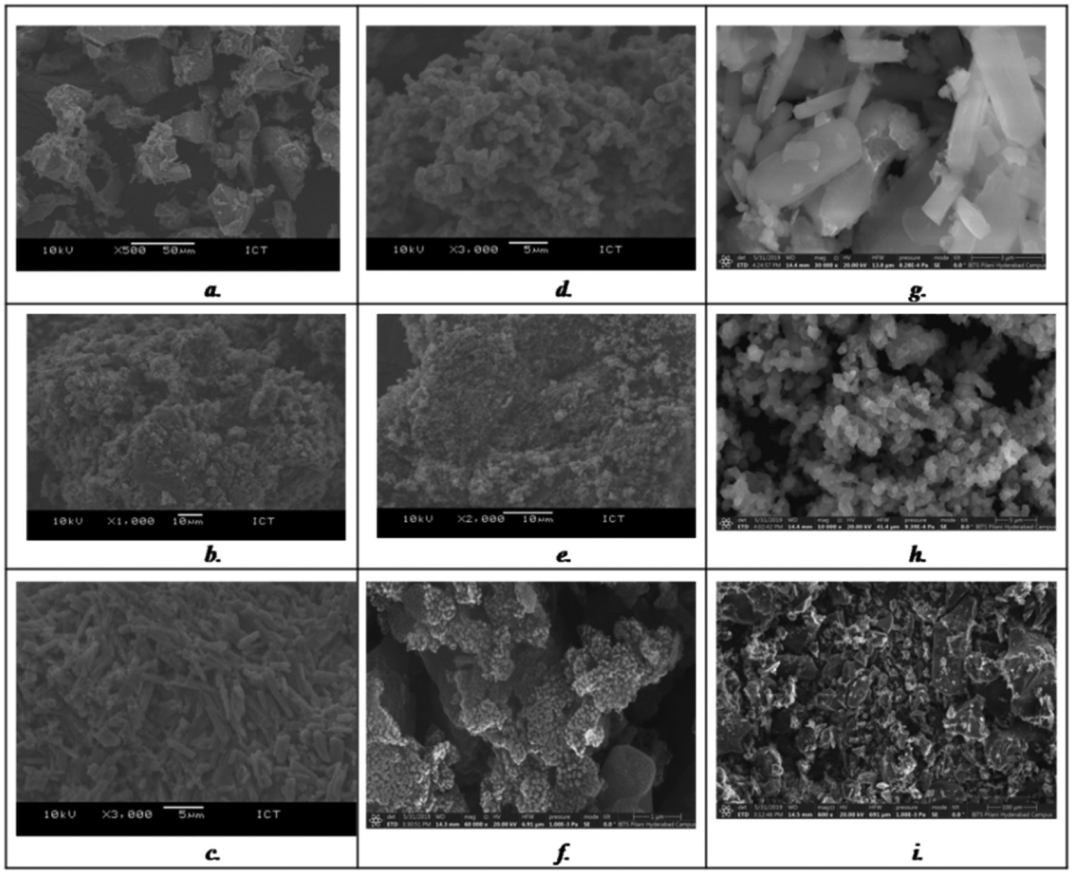


**Figure 3.** SEM images of(a) $TiO_2$, (b) Polyaniline(PANi), (c) Polythiophene (PTh), (d) Polypyrrole (PPy), (e) Polyindole (Pin), (f) $TiO_2$-Polyaniline composite (Ti-PANi), (g) $TiO_2$-Polythiophene composite (Ti-PTh), (h) $TiO_2$-Polypyrrole composite (Ti-PPy) and (i) $TiO_2$-Polyindole composite (Ti-Pin).

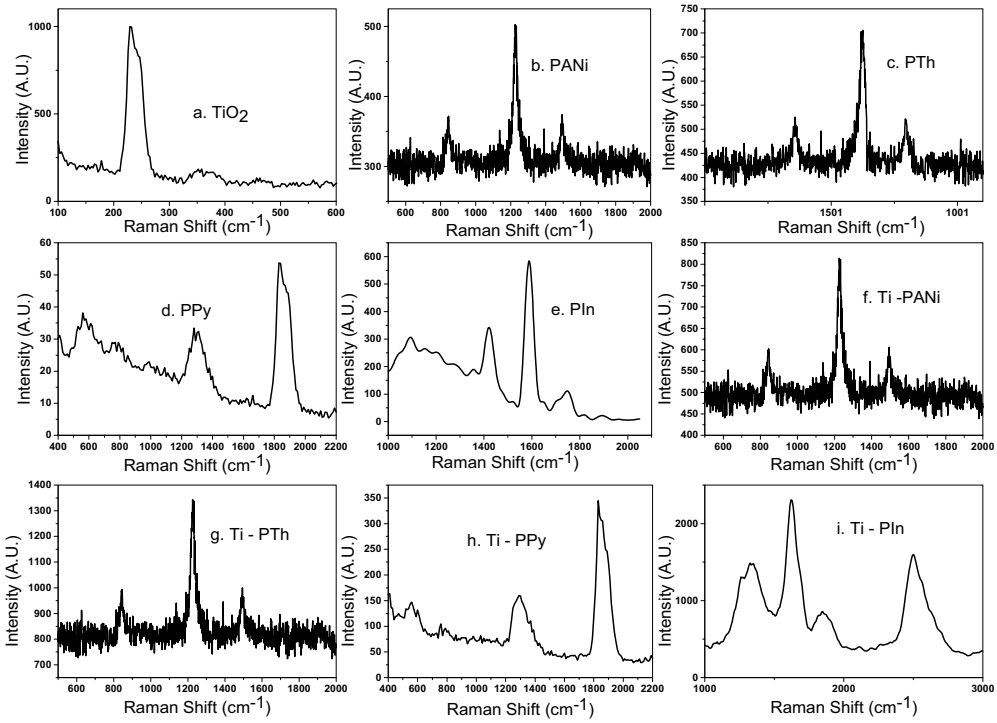


**Figure 4.** Raman Spectra of (a) $TiO_2$, (b) Polyaniline(PANi), (c) Polythiophene (PTh), (d) Polypyrrole (PPy), (e) Polyindole (Pin), (f) $TiO_2$-Polyaniline composite (Ti-PANi), (g) $TiO_2$-Polythiophene composite (Ti-PTh), (h) $TiO_2$-Polypyrrole composite (Ti-PPy) and (i) $TiO_2$-Polyindole composite (Ti-PIn).

near 1500 $cm^{-1}$ is a characteristic feature of the Raman spectra of aromatic and heteroaromatic systems. It is reported as very strong and dominating in the whole Raman spectrum. While it shifts toward lower frequencies with an increase in chain length. It shows somewhat variation in frequencies from one chemical series to another within the class of oligo and polythiophenes, but within individual class it is almost invariably strong and unshifted. Some signals appearing at the lower frequency side shows intensity enhancement with increase in chain length.[35]

Polypyrrole signal at 1330 $cm^{-1}$ corresponds to C–C stretching in ring and antisymmetric C–N stretching.[36] Polyindole signal 1102 is due to out-of-plane as well as in-plane deformation of N-H, peak near 1594 is because of C = C backbone stretching and peak at 1414 correspond to ring stretching.[37,38] Ti-PANi and Ti-PPy composites show the same peak as polymer. Ti-PIn and Ti-PTh show shifting of peaks. Peaks observed in composites indicate strong interaction between $TiO_2$ and polymers.

### 3.4. UV spectroscopy

Figure 5 shows UV-Visible spectra of (a) $TiO_2$, (b) Polyaniline (PANi), (c) Polythiophene (PTh), (d) Polypyrrole (PPy), (e) Polyindole (Pin), (f) $TiO_2$-Polyaniline composite (Ti-PANi), (g) $TiO_2$-Polythiophene composite (Ti-PTh), (h) $TiO_2$-Polypyrrole composite (Ti-PPy) and (i) $TiO_2$-Polyindole composite (Ti-Pin). Band gap and absorption peak values for $TiO_2$, Polymers and their composites are shown in Table 2.

In the present work, UV-VIS technique was used to study the absorption wavelengths of materials and band gap. The absorption study of samples under study was recorded using Agilent Cary 60 UV–VIS spectrophotometer.

The energy band gap of sample can be calculated using relations: $E = hc/\lambda$[39]

Where Energy (E) = Band gap, Planks constant (h) = $6.626 \times 10^{-34}$ Joules sec,

Velocity of Light (c) = $2.99 \times 10^{8}$ meter/sec and Wavelength ($\lambda$) = Absorption peak value. Also, 1 eV = $1.6 \times 10^{-19}$ Joules (Conversion factor)

### 3.5. Photo luminescence

Figure 6 shows Photoluminescence (PL) spectra of (a) $TiO_2$, (b) Polyaniline(PANi), (c) Polythiophene (PTh), (d) Polypyrrole (PPy), (e) Polyindole (Pin), (f) $TiO_2$-Polyaniline composite (Ti-PANi), (g) $TiO_2$-Polythiophene composite (Ti-PTh), (h) $TiO_2$-Polypyrrole composite (Ti-PPy) and (i) $TiO_2$-Polyindole composite (Ti-Pin).

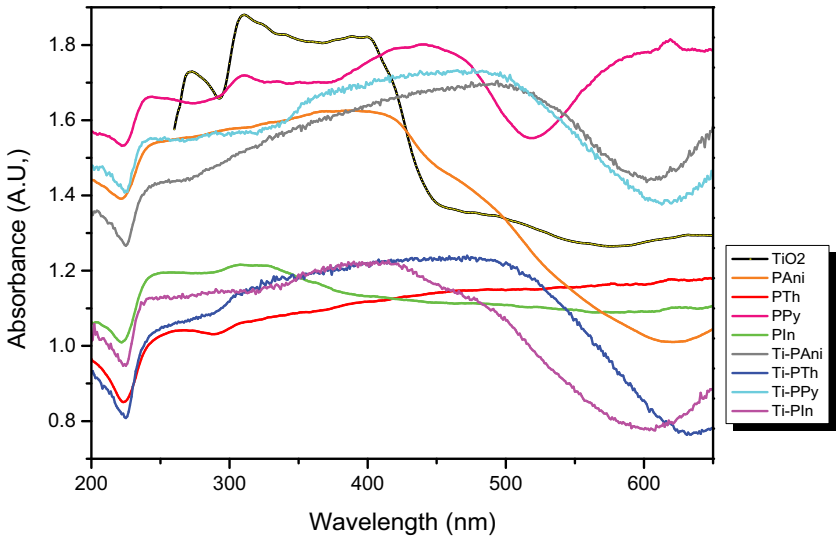


**Figure 5.** UV-Visible spectra of (a) $TiO_2$, (b) Polyaniline(PANi), (c) Polythiophene (PTh), (d) Polypyrrole (PPy), (e) Polyindole (Pin), (f) $TiO_2$-Polyaniline composite (Ti-PANi), (g) $TiO_2$-Polythiophene composite (Ti-PTh), (h) $TiO_2$-Polypyrrole composite (Ti-PPy) and (i) $TiO_2$-Polyindole composite (Ti-Pin).

**Table 2.** Band gap and absorption peak values for $TiO_2$, polymers and their composites.

| Compound | Absorption peak value (Wavelength in nm) | Band gap (eV) |
|---|---|---|
| 1. $TiO_2$ | 350 | 3.54 |
| 2. Polyaniline(PANi) | 310 | 3.99 |
| 4. Polythiophene(PTh) | 265 | 4.67 |
| 3. Polypyrrole (PPy) | 440 | 2.82 |
| 5. Polyindole(Pin) | 249 | 4.98 |
| 6. $TiO_2$-Polyaniline composite(Ti-PANi) | 450 | 2.8 |
| 8. $TiO_2$-Polythiophene composite(Ti-PTh) | 400 | 3.1 |
| 7. $TiO_2$-Polypyrrole composite(Ti-PPy) | 450 | 2.8 |
| 9. $TiO_2$-Polyindole composite(Ti-Pin) | 400 | 3.1 |

$TiO_2$ shows PL signal near 490 nm.[40–42] Polyaniline shows peak at 367 nm, due to $\pi \rightarrow \pi^*$ transition.[43] Polythiophene shows absorption peak near excitation wavelength 325 nm.[44] PL signal for polyindole comes from the recombination of electron in singly occupied oxygen vacancies with photo excited holes.[45,46] Polypyrrole shows PL emission peaks near 400 nm. However, agglomeration affects the PL intensity of the polymer.[47] This PL emission characteristics indicate the promise of the synthesized materials for practical applications in ultraviolet and visible light emission devices.

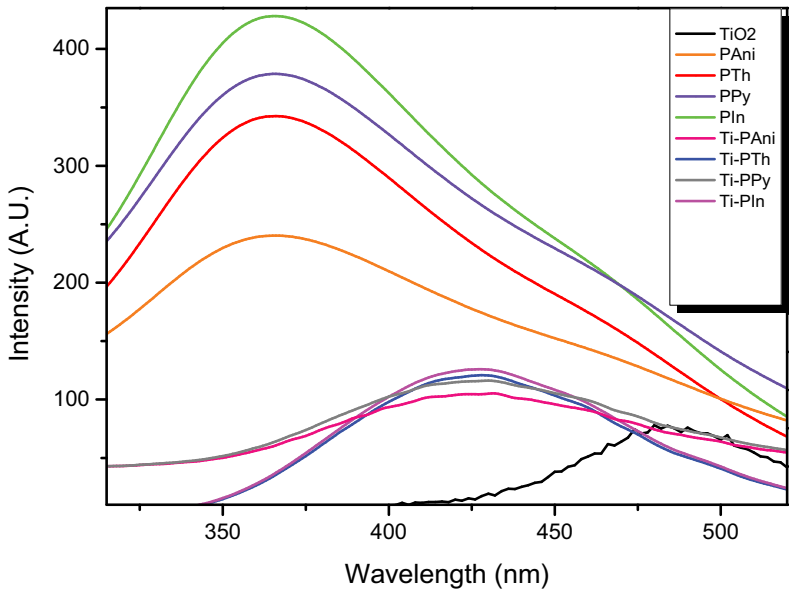


**Figure 6.** Photoluminescence(PL) spectra of (a) $TiO_2$, (b) Polyaniline(PANi), (c) Polythiophene (PTh), (d) Polypyrrole (PPy), (e) Polyindole (Pin), (f) $TiO_2$-Polyaniline composite (Ti-PANi), (g) $TiO_2$-Polythiophene composite (Ti-PTh), (h) $TiO_2$-Polypyrrole composite (Ti-PPy) and (i) $TiO_2$-Polyindole composite (Ti-Pin).

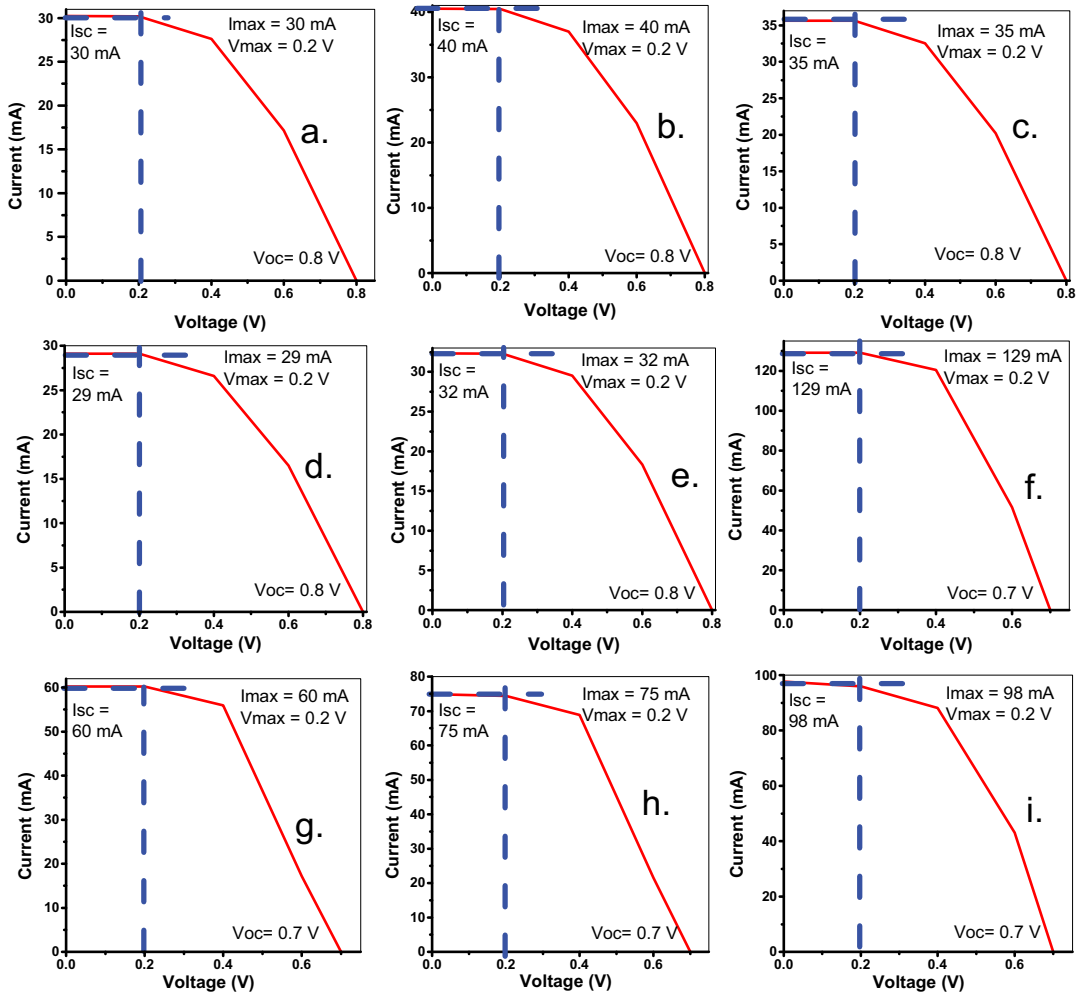


**Figure 7.** PV response of (a) $TiO_2$, (b) Polyaniline(PANi), (c) Polythiophene (PTh), (d) Polypyrrole (PPy), (e) Polyindole (PIn), (f) $TiO_2$-Polyaniline composite (Ti-PANi), (g) $TiO_2$-Polythiophene composite (Ti-PTh), (h) $TiO_2$-Polypyrrole composite (Ti-PPy) and (i) $TiO_2$-Polyindole composite (Ti-PIn).

**Table 3.** PV parameters (where Pin = 0.25 W/m$^2$).

| Compound | Imax (mA) | Vmax (V) | Isc (mA) | Voc (V) | $FF = \frac{I_{MAX} \times V_{MAX}}{I_{SC} \times V_{OC}}$ | $\%\eta = \left(\frac{I_{SC} \times V_{OC} \times FF}{P_{in}}\right) \times 100$ |
|---|---|---|---|---|---|---|
| (a) $TiO_2$ | 30 | 0.2 | 30 | 0.8 | 0.25 | 2.4 |
| (b) Polyaniline(PANi) | 40 | 0.2 | 40 | 0.8 | 0.25 | 3.2 |
| (c) Polythiophene (PTh) | 35 | 0.2 | 35 | 0.8 | 0.25 | 2.8 |
| (d) Polypyrrole (PPy) | 29 | 0.2 | 29 | 0.8 | 0.25 | 2.32 |
| (e) Polyindole (PIn) | 32 | 0.2 | 32 | 0.8 | 0.25 | 2.56 |
| (f) $TiO_2$-Polyaniline composite (Ti-PANi) | 129 | 0.2 | 129 | 0.7 | 0.29 | 10.47 |
| (g) $TiO_2$-Polythiophene composite (Ti-PTh) | 60 | 0.2 | 60 | 0.7 | 0.29 | 4.872 |
| (h) $TiO_2$-Polypyrrole composite (Ti-PPy) | 75 | 0.2 | 75 | 0.7 | 0.29 | 6.09 |
| (i) $TiO_2$-Polyindole composite (Ti-PIn) | 98 | 0.2 | 98 | 0.7 | 0.29 | 7.957 |

### 3.6. Measurements of photovoltaic characteristics

Figure 7a–i represents Current-Voltage (IV) characteristics of fabricated photovoltaic cell (a) $TiO_2$, (b) Polyaniline(PANi), (c) Polythiophene (PTh), (d) Polypyrrole (PPy), (e) Polyindole (PIn), (f) $TiO_2$ Polyaniline composite (Ti-PANi), (g) TiO2-Polythiophene composite (Ti-PTh), (h) TiO2-Polypyrrole composite (Ti-PPy) and (i) TiO2-Polyindole composite (Ti-PIn) respectively. The photovoltaic parameters of these materials are listed in Table 3. It is observed that TiO2-Polyaniline composite (Ti-PANi) shows higher short

circuit current (Isc) ascompared to all other mentioned materials.

The Current-Voltage (I–V) characteristics of PANI-TiO2 heterostructure diode show a nonlinear behavior. It indicates that a *p*–n heterostructure at PANI-TiO2 interface has been generated. The doping of TiO2 nanoparticles which facilitates the formation of a more efficient network for charge transport. Consequently, the conductivity of nanocomposites also increases with the addition of TiO2. It also facilitates interchain conduction due to the formation of conducting pathways between the chains. Thus, by the addition of TiO2, there becomes a more efficient network for charge transport in the PANI matrix which leads to higher conductivities. As a result, dispersion capacity of TiO2-Polyaniline composite (Ti-PANi) and charge transfer phenomenon are significantly enhancing due to synergistic effects in composite which leads to higher values of Isc.[48–51] The significant enhancement in the value of % η is due to the addition of TiO2 in PANi in composite. The maximum value of % η is found to be 10.47% for TiO2-Polyaniline composite (Ti-PANi).

## 4. Conclusion

In summary, $TiO_2$, four Polymers (Polyaniline, Polythiophene, Polypyrrole, Polyindole) and their four composites ($TiO_2$-Polyaniline composite, $TiO_2$-Polythiophene composite, $TiO_2$-Polypyrrole composite, $TiO_2$-Polyindole composite) were prepared. PV performance of all above compounds were studied. The significant enhancement in value of % η takes place by the addition of $TiO_2$ in PANi during preparation of composite. The value of % η is found to be highest for $TiO_2$-Polyaniline composite (Ti-PANi)i.e.10.47%.

## Notes on contributors

***Ms. Bhagyashri U.Tale*** is Ph.D. student, at department of chemistry, Bajaj College of Science, Dist.Wardha, Maharashtra, India.

***Dr. K.R. Nemade*** is Assistant Professor, at department of physics, Indira Mahavidyalaya, Kalamb,Dist. yavatmal, Maharashtra, India.

***Dr. P.V. Tekade*** is Associate Professor, at department of chemistry, Bajaj College of Science, Dist.Wardha, Maharashtra, India.

## References

[1] Mahmood, N.; Zhang, C.; Yin, H.; Hou, Y. Graphene-based Nanocomposites for Energy Storage and Conversion in Lithium Batteries, Supercapacitors and Fuel Cells. *J. Mater. Chem. A* 2014, *2*(1), 15–32. DOI: 10.1039/C3TA13033A.

[2] Jordehi, A. R. Parameter Estimation of Solar Photovoltaic (PV) Cells: A Review. *Renewable Sustainable Energy Rev.* 2016, *61*, 354–371. DOI: 10.1016/j.rser.2016.03.049.

[3] Bai, J.; Liu, S.; Hao, Y.; Zhang, Z.; Jiang, M.; Zhang, Y. Development of a New Compound Method to Extract the Five Parameters of PV Modules. *Energy Conversion Manage.* 2014, *79*, 294–303. DOI: 10.1016/j.enconman.2013.12.041.

[4] Shafiee, S.; Topal, E. When Will Fossil Fuel Reserves Be Diminished? *Energy Policy*. 2009, *37*(1), 181–189. DOI: 10.1016/j.enpol.2008.08.016.

[5] Apergis, N.; Payne, J. E. Renewable Energy, Output, CO2 Emissions, and Fossil Fuel Prices in Central America: Evidence from a Nonlinear Panel Smooth Transition Vector Error Correction Model. *Energy Econ.* 2014, *42*, 226–232. DOI: 10.1016/j.eneco.2014.01.003.

[6] Shivalkar, R. S.; Jadhav, H. T.; Deo, P. Feasibility Study for the Net Metering Implementation in Rooftop Solar PV Installations across Reliance Energy Consumers. 2015 International Conference on Circuits, Power and Computing Technologies [ICCPCT-2015], IEEE: Nagercoil, India, Mar, 2015, pp 1–6.

[7] Wang, Y.; Zhou, S.; Huo, H. Cost and CO2 Reductions of Solar Photovoltaic Power Generation in China: Perspectives for 2020. *Renewable Sustainable Energy Rev.* 2014, *39*, 370–380. DOI: 10.1016/j.rser.2014.07.027.

[8] Sundareswaran, K.; Sankar, P.; Nayak, P. S. R.; Simon, S. P.; Palani, S. Enhanced Energy Output from a PV System under Partial Shaded Conditions through Artificial Bee Colony. *IEEE Trans. Sustainable Energy*. 2014, *6*(1), 198–209. DOI: 10.1109/TSTE.2014.2363521.

[9] Trifunović, M. Energy at the Crossroads. Synthesis 2015-International Scientific Conference of IT and Business-Related Research, Singidunum University: Serbia, 2015, pp 186–190.

[10] Hunt, T. *The Solar Singularity Is Nigh*; Greentech Media, (accessed 29, 2015).

[11] Liu, Z.; Zhou, J.; Xue, H.; Shen, L.; Zang, H.; Chen, W. Polyaniline/TiO2 Solar Cells. *Synth. Met.* 2006, *156*(9–-10), 721–723. DOI: 10.1016/j.synthmet.2006.04.001.

[12] Breeze, A. J.; Schlesinger, Z.; Carter, S. A.; Brock, P. J. Charge Transport in TiO 2/M E H– P P V Polymer Photovoltaics. *Phys. Rev. B*. 2001, *64*(12), 125205. DOI: 10.1103/PhysRevB.64.125205.

[13] Arango, A. C.; Johnson, L. R.; Bliznyuk, V. N.; Schlesinger, Z.; Carter, S. A.; Hörhold, H. H. Efficient Titanium Oxide/conjugated Polymer Photovoltaics for Solar Energy Conversion. *Adv.Mate.* 2000, *12*(22), 1689–1692. DOI: 10.1002/1521-4095(200011)12:22<1689::AID-ADMA1689>3.0.CO;2-9.

[14] Kawata, K.; Gan, S. N.; Ang, D. T. C.; Sambasevam, K. P.; Phang, S. W.; Kuramoto, N. Preparation of polyaniline/TiO2 Nanocomposite Film with Good Adhesion Behavior for Dye-sensitized Solar Cell Application. *Polym. Compos.* 2013, *34*(11), 1884–1891. DOI: 10.1002/pc.22595.

[15] Bouclé, J.; Ravirajan, P.; Nelson, J. Hybrid Polymer–metal Oxide Thin Films for Photovoltaic Applications.

*J. Mater. Chem.* 2007, *17*(30), 3141–3153. DOI: 10.1039/b706547g.

[16] Çetin, H.; Boyarbay, B.; Akkaya, A.; Uygun, A.; andAyyildiz, E. N. İ. S. E. Electrical Characterization of Heterojunction between Polyaniline Titanium Dioxide Tetradecyltrimethylammonium Bromide and N-silicon. *Synth. Met.* 2011, *161*(21–22), 2384–2389. DOI: 10.1016/j.synthmet.2011.09.005.

[17] Ameen, S.; Akhtar, M. S.; Kim, Y. S.; Shin, H. S. *Fabrication, Doping and Characterization of Polyaniline and Metal Oxides: Dye Sensitized Solar Cells*; Solar cells-dye-sensitized devices, 2011.

[18] Bahramian, A.; Vashaee, D. In-situ Fabricated Transparent Conducting Nanofiber-shape Polyaniline/coral-like TiO2 Thin Film: Application in Bifacial Dye-sensitized Solar Cells. *Solar Energy Mater. Solar Cells*. 2015, *143*, 284–295. DOI: 10.1016/j.solmat.2015.07.011.

[19] Chung, I.; Lee, B.; He, J.; Chang, R. P.; Kanatzidis, M. G. All-solid-state Dye-sensitized Solar Cells with High Efficiency. *Nature*. 2012, *485*, 486. DOI: 10.1038/nature11067.

[20] Jing, X.; Wang, Y.; Wu, D.; Qiang, J. Sonochemical Synthesis of Polyaniline Nanofibers. *Ultrason. Sonochem.* 2007, *14*(1), 75–80. DOI: 10.1016/j.ultsonch.2006.02.001.

[21] Tat'yana, V. V.; Efimov, O. N. Polypyrrole: A Conducting Polymer; Its Synthesis, Properties and Applications. *Russ. Chem. Rev.* 1997, *66*(5), 443. DOI: 10.1070/RC1997v066n05ABEH000261.

[22] Wadatkar, N. S.; Waghuley, S. A. Complex Optical Studies on Conducting Polyindole As-synthesized through Chemical Route. *Egypt. J. Basic Appl. Sci.* 2015, *2*(1), 19–24. DOI: 10.1016/j.ejbas.2014.12.006.

[23] Wadatkar, N. S.; Waghuley, S. A. Studies on Properties of As-synthesized Conducting Polythiophene through Aqueous Chemical Route. *J. Mater. Sci.: Mater. Electron.* 2016, *27*(10), 10573–10581.

[24] Molea, A.; Popescu, V. The Obtaining of Titanium Dioxide Nanocrystalline Powders. *Optoelectron. Adv. Mater. Rapid Commun.* 2011, *5*(3–4), 242–246.

[25] Theivasanthi, T.; Alagar, M. Titanium Dioxide (Tio2) Nanoparticles XRD Analyses: An Insight. *arXiv preprint arXiv:1307*.1091. 2013.

[26] Rajakani, P.; Vedhi, C. Electrocatalytic Properties of polyaniline–TiO2 Nanocomposites. *Int. J. Ind. Chem.* 2015, *6*(4), 247–259. DOI: 10.1007/s40090-015-0046-8.

[27] Bhagwat, A. D.; Sawant, S. S.; Mahajan, C. M. *Facile Rapid Synthesis of Polyaniline (Pani) Nanofibers*, 2016.

[28] Sakthivel, S.; Boopathi, A. Synthesis and Preparation of Polythiophene Thin Film by Spin Coating Method. *Int. J. Sci. Res. Sec.* 2014, *141*, 97–100.

[29] Ma, C.; Sg, P.; Pr, G.; Shashwati, S. Synthesis and Characterization of Polypyrrole (Ppy) Thin Films. *Soft Nanosci. Lett.* 2011, *2011*,6–10.

[30] Sathiyanarayanan, S.; Azim, S. S.; Venkatachari, G. Preparation of polyaniline–TiO2 Composite and Its Comparative Corrosion Protection Performance with Polyaniline. *Synth. Met.* 2007, *157*(4–5), 205–213. DOI: 10.1016/j.synthmet.2007.01.012.

[31] Nemade, K. R.; Waghuley, S. A. Low Temperature Synthesis of Semiconducting α-Al2O3 Quantum Dots. *Ceram. Int.* 2014, *40*(4), 6109–6113. DOI: 10.1016/j.ceramint.2013.11.062.

[32] Balachandran, U. G. E. N.; Eror, N. G. Raman Spectra of Titanium Dioxide. *J. Solid State Chem.* 1982, *42*(3), 276–282. DOI: 10.1016/0022-4596(82)90006-8.

[33] Frank, O.; Zukalova, M.; Laskova, B.; Kürti, J.; Koltai, J.; Kavan, L. Raman Spectra of Titanium Dioxide (Anatase, Rutile) with Identified Oxygen Isotopes (16, 17, 18). *Phys. Chem. Chem. Phys.* 2012, *14*(42), 14567–14572. DOI: 10.1039/c2cp42763j.

[34] Mažeikienė, R.; Tomkutė, V.; Kuodis, Z.; Niaura, G.; Malinauskas, A. Raman Spectroelectrochemical Study of Polyaniline and Sulfonated Polyaniline in Solutions of Different pH. *Vib. Spectrosc.* 2007, *44*(2), 201–208. DOI: 10.1016/j.vibspec.2006.09.005.

[35] Agosti, E.; Rivola, M.; Hernandez, V.; Del Zoppo, M.; Zerbi, G. Electronic and Dynamical Effects from the Unusual Features of the Raman Spectra of Oligo and Polythiophenes. *Synth. Met.* 1999, *100*(1), 101–112. DOI: 10.1016/S0379-6779(98)00167-2.

[36] Šetka, M.; Calavia, R.; Vojkůvka, L.; Llobet, E.; Drbohlavová, J.; Vallejos, S. Raman and XPS Studies of Ammonia Sensitive Polypyrrole Nanorods and Nanoparticles. *Sci. Rep.* 2019, *9*(1), 1–10. DOI: 10.1038/s41598-019-44900-1.

[37] Raj, R. P.; Ragupathy, P.; Mohan, S. Remarkable Capacitive Behavior of a Co3O 4–polyindole Composite as Electrode Material for Supercapacitor Applications. *J. Mater. Chem. A*. 2015, *3*(48), 24338–24348. DOI: 10.1039/C5TA07046E.

[38] Liu, Y. C.; Hwang, B. J.; Jian, W. J.; Santhanam, R. In Situ Cyclic Voltammetry-surface-enhanced Raman Spectroscopy: Studies on the Doping–undoping of Polypyrrole Film. *Thin Solid Films*. 2000, *374*(1), 85–91. DOI: 10.1016/S0040-6090(00)01061-0.

[39] Nemade, K. R.; Waghuley, S. A. UV–VIS Spectroscopic Study of One Pot Synthesized Strontium Oxide Quantum Dots. *Results Phys.* 2013, *3*, 52–54. DOI: 10.1016/j.rinp.2013.03.001.

[40] Brüninghoff, R.; Wenderich, K.; Korterik, J. P.; Mei, B. T.; Mul, G.; Huijser, A. Time-Dependent Photoluminescence of Nanostructured Anatase TiO2 and the Role of Bulk and Surface Processes. *J. Phys. Chem. C*. 2019, *123*(43), 26653–26661. DOI: 10.1021/acs.jpcc.9b06890.

[41] Xiao, Q.; Si, Z.; Yu, Z.; Qiu, G. Sol–gel Auto-combustion Synthesis of Samarium-doped TiO2 Nanoparticles and Their Photocatalytic Activity under Visible Light Irradiation. *Mater. Sci. Eng.* 2007, *137*(1–3), 189–194. DOI: 10.1016/j.mseb.2006.11.011.

[42] Haque, F. Z.; Nandanwar, R.; Singh, P. Evaluating Photodegradation Properties of Anatase and Rutile TiO2 Nanoparticles for Organic Compounds. *Optik*. 2017, *128*, 191–200. DOI: 10.1016/j.ijleo.2016.10.025.

[43] Chatterjee, M. J.; Ghosh, A.; Mondal, A.; Banerjee, D. Polyaniline–single Walled Carbon Nanotube Composite–a Photocatalyst to Degrade Rose Bengal and Methyl Orange Dyes under Visible-light Illumination. *RSC Adv.* 2017, *7*(58), 36403–36415. DOI: 10.1039/C7RA03855K.

[44] Tripathi, A.; Mishra, S. K.; Bahadur, I.; Shukla, R. K. Optical Properties of Regiorandom polythiophene/

Al2O3 Nanocomposites and Their Application to Ammonia Gas Sensing. *J. Mater. Sci.: Mater. Electron.* 2015, *26*(10), 7421–7430.

[45] Vanheusden, K.; Warren, W. L.; Seager, C. H.; Tallant, D. R.; Voigt, J. A.; Gnade, B. E. Mechanisms behind Green Photoluminescence in ZnO Phosphor Powders. *J. Appl. Phys.* 1996, *79*(10), 7983–7990. DOI: 10.1063/1.362349.

[46] Vanheusden, K.; Seager, C. H.; Warren, W. T.; Tallant, D. R.; Voigt, J. A. Correlation between Photoluminescence and Oxygen Vacancies in ZnO Phosphors. *Appl. Phys. Lett.* 1996, *68*(3), 403–405. DOI: 10.1063/1.116699.

[47] Dey, S.; Kar, A. K. Morphological and Optical Properties of Polypyrrole Nanoparticles Synthesized by Variation of Monomer to Oxidant Ratio. *Mater. Today Proc.* 2019, *18*, 1072–1076.

[48] Nemade, K.; Dudhe, P.; Tekade, P. Enhancement of Photovoltaic Performance of Polyaniline/graphene Composite-based Dye-sensitized Solar Cells by Adding TiO2 Nanoparticles. *Solid State Sci.* 2018, *83*, 99–106. DOI: 10.1016/j.solidstatesciences.2018.07.009.

[49] Zhang, X.; Yan, G.; Ding, H.; Shan, Y. Fabrication and Photovoltaic Properties of Self-assembled Sulfonated polyaniline/TiO2 Nanocomposite Ultrathin Films. *Mater. Chem. Phys.* 2007, *102*(2–3), 249–254. DOI: 10.1016/j.matchemphys.2006.12.013.

[50] Abaci, S.; Nessark, B.; Riahi, F. Preparation and Characterization of Polyaniline+ TiO 2 Composite Films. *Ionics*. 2014, *20*(12), 1693–1702. DOI: 10.1007/s11581-014-1129-9.

[51] Deivanayaki, S.; Ponnuswamy, V.; Ashokan, S.; Jayamurugan, P.; Mariappan, R. Synthesis and Characterization of TiO2-doped Polyaniline Nanocomposites by Chemical Oxidation Method. *Mater. Sci. Semicond. Process.* 2013, *16*(2), 554–559. DOI: 10.1016/j.mssp.2012.07.004.